

Practical second-order inelastic analysis for three-dimensional steel frames subjected to distributed load

Seung-Eock Kim^{a,*}, Se-Hyu Choi^b

^a*Department of Civil and Environmental Eng., Construction Tech. Research Institute, Sejong University,
98 Kunja-dong, Kwangjin-ku, 143 747 Seoul, South Korea*

^b*Department of Civil Engineering, Kyungpook National University, Daegu, 702-701, South Korea*

Received 9 October 2003; accepted 26 July 2004

Available online 27 October 2004

Abstract

A practical second-order inelastic analysis of three-dimensional steel frames subjected to distributed load is developed. This analysis realistically assesses both strength and behavior of a structural system and its component members in a direct manner. To capture second-order effects associated with $P-\delta$ and $P-\Delta$, stability functions are used to minimize modeling and solution time. The Column Research Council (CRC) tangent modulus concept is used to account for gradual yielding due to residual stresses. A softening plastic hinge model is used to represent the degradation from elastic to zero stiffness associated with development of a hinge. In proposed analysis, a member has two elements and three nodal points. A plastic hinge location can be captured in analysis as the internal nodal point traces the maximum moment location at each load step. Maximum moments and load-displacements predicted by the proposed analysis compare well with those given by other approaches. © 2004 Elsevier Ltd. All rights reserved.

Keywords: Second-order inelastic analysis; Geometric nonlinearity; Material nonlinearity; Stability function; Distributed load; Steel frame

* Corresponding author. Tel./fax: +82 2 3408 3332.

E-mail address: sekim@sejong.ac.kr (S.-E. Kim).

1. Introduction

Over the past twenty years, many researchers have developed and validated various methods of performing second-order inelastic analyses on steel frames. Most of these studies may be categorized into one of two types: (1) plastic-zone; or (2) plastic-hinge, based on the degree of refinement used to represent yielding. The plastic-zone method uses the highest refinement while the elastic–plastic hinge method allows for a significant simplification.

In the plastic-zone method, a frame member is discretized into finite elements, and the cross-section of each finite element is subdivided into many fibers [1–4]. The deflection at each division along the member is obtained by numerical integration. The incremental load-deflection response at each load step, with updated geometry, captures the second-order effects. The residual stress in each fiber is assumed constant since the fibers are sufficiently small. The stress state of each fiber can be explicitly determined, and the gradual spread of yielding traced. A plastic-zone analysis eliminates the need for separate member capacity checks since second-order effects, the spread of plasticity, and residual stresses are accounted for directly. As a result, a plastic-zone solution is considered ‘exact.’ Although the plastic-zone solution may be considered ‘exact,’ it is not conducive to daily use in engineering design, because it is too computationally intensive and too costly.

A more simple and efficient way to represent inelasticity in frames is the elastic–plastic hinge method. Here the element remains elastic except at its ends where zero-length plastic hinges form. This method accounts for inelasticity but not the spread of yielding through the section or between the hinges. The effect of residual stresses between hinges is not accounted for either. The geometric nonlinearities are considered by stability functions using only one beam-column element to define the second-order effect of an individual member so that they are an efficient and economical method in frame analysis. The elastic–plastic hinge method has distinct advantage over the plastic-zone method for slender members (whose dominant mode of failure is elastic instability) as it compares well with plastic-zone solutions. However, for stocky members (which sustain significant yielding), it over-predicts the capacity of members as it neglects to consider the gradual reduction of stiffness as yielding progresses through and along the member. Consequently, modifications must be made before this method can be proposed for a wide range of framed structures.

The refined plastic-hinge analysis, based on simple refinements of the elastic–plastic hinge model, has been proposed for plane frame analysis in recent works [5–13]. The analysis overcomes difficulty of the elastic–plastic hinge method. Orbison, Prakash and Powell and Liew and Tang [14–16], and Kim et al. (2000) have proposed for second-order inelastic analysis methods for the three-dimensional structures. However, these analysis methods are based on the assumption that the plastic hinge occurs only at the member ends. When a member is subjected to distributed loads, a plastic hinge may occur within the member as well as at the member ends. The assumption that the plastic hinge occurs only at the member ends is no longer valid. Wong [17] has introduced a moving node tracing the location of the internal plastic hinge which is the location of maximum bending moment. However, Wong’s method uses an elasto-plastic analysis ignoring geometric nonlinear effects. The exact location of the internal plastic hinge should be calculated considering not only inelasticity but also second-order ($P-\delta$) effect.

In this paper, a practical second-order inelastic analysis of three-dimensional steel frame subjected to linearly varying distributed lateral loads is developed. The material nonlinearity is considered by using CRC tangent modulus and a parabolic function. The geometric nonlinearity is considered by stability functions accounting for the interaction between axial force and bending moment. The internal nodal point traces the maximum moment location at each load step so that a plastic hinge location can be captured in analysis.

2. Practical second-order inelastic analysis

A practical second-order inelastic analysis of three-dimensional steel frames subjected to linearly varying distributed lateral loads will be presented. This analysis accounts for both geometric and material nonlinearities. The geometric nonlinearities include $P-\delta$ effect and $P-\Delta$ effect. Stability functions are used to account for $P-\delta$ effect indicating additional moment induced by the axial force applied on a deflected member. Element stiffness matrix take into account $P-\Delta$ effect indicating additional moment produced by the gravity loads applied on the swayed frame. The material nonlinearities include gradual yielding of steel associated with flexure and residual stresses. The moving node concept is used to trace the plastic hinge location within a member.

2.1. Basic assumptions

The following assumptions are used for modeling of a beam-column element.

- (1) All elements are initially straight and prismatic. Plane cross-section remains plane after deformation.
- (2) Local buckling and lateral-torsional buckling are not considered. All members are assumed to be fully compact and adequately braced.
- (3) Large displacements are allowed, but strains are small.
- (4) The element stiffness formulation is based on beam-column stability functions considering axial and bending deformations.
- (5) Strain hardening is not considered. Plastic hinges cannot sustain additional loads.
- (6) Reduction of torsional and shear stiffnesses is not considered in plastic hinge.

2.2. Planar beam-column subjected to distributed lateral loads

Considering the prismatic beam-column element subjected to linearly varying distributed lateral loads as incremental in Fig. 1, the incremental force-displacement relationship of this element may be written as

$$\begin{Bmatrix} \dot{M}_A \\ \dot{M}_B \\ \dot{P} \end{Bmatrix} = \frac{EI}{L} \begin{bmatrix} S_1 & S_2 & 0 \\ S_2 & S_1 & 0 \\ 0 & 0 & \frac{A}{I} \end{bmatrix} \begin{Bmatrix} \dot{\theta}_A \\ \dot{\theta}_B \\ \dot{\delta} \end{Bmatrix} + \begin{Bmatrix} \dot{M}_{FA} \\ \dot{M}_{FB} \\ 0 \end{Bmatrix} \quad (1)$$

where

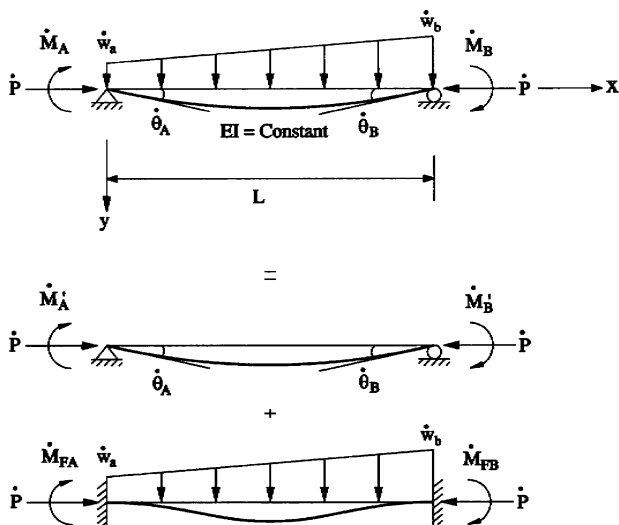


Fig. 1. Beam-column subjected to incremental distributed lateral load.

\dot{M}_A, \dot{M}_B	incremental end moments
\dot{P}	incremental axial force
S_1, S_2	stability functions
$\dot{\theta}_A, \dot{\theta}_B$	incremental joint rotations
$\dot{\delta}$	incremental axial displacement
$\dot{M}_{FA}, \dot{M}_{FB}$	incremental fixed-end moments
A, I, L	area, moment of inertia, and length of beam-column element
E	modulus of elasticity.

2.3. Stability functions accounting for $P-\delta$ effect

To capture $P-\delta$ effects, stability functions are used to minimize modeling and solution time. Generally only one or two elements are needed per member. The simplified stability functions reported by [18] are used here. The stability functions given by Eq. (1) may be written as

$$S_1 = \begin{cases} \frac{\pi\sqrt{\rho}\sin(\pi\sqrt{\rho}) - \pi^2\rho\cos(\pi\sqrt{\rho})}{2 - 2\cos(\pi\sqrt{\rho}) - \pi\sqrt{\rho}\sin(\pi\sqrt{\rho})} & \text{if } P < 0 \\ \frac{\pi^2\rho\cosh(\pi\sqrt{\rho}) - \pi\sqrt{\rho}\sinh(\pi\sqrt{\rho})}{2 - 2\cosh(\pi\sqrt{\rho}) + \pi\sqrt{\rho}\sinh(\pi\sqrt{\rho})} & \text{if } P > 0 \end{cases} \quad (2)$$

$$S_2 = \begin{cases} \frac{\pi^2\rho - \pi\sqrt{\rho}\sin(\pi\sqrt{\rho})}{2 - 2\cos(\pi\sqrt{\rho}) - \pi\sqrt{\rho}\sin(\pi\sqrt{\rho})} & \text{if } P < 0 \\ \frac{\pi\sqrt{\rho}\sinh(\pi\sqrt{\rho}) - \pi^2\rho}{2 - 2\cosh(\pi\sqrt{\rho}) + \pi\sqrt{\rho}\sinh(\pi\sqrt{\rho})} & \text{if } P > 0 \end{cases} \quad (3)$$

where $\rho = P/(\pi^2 EI/L^2)$, P is positive in tension.

The numerical solutions obtained from Eqs. (2) and (3) are indeterminate when the axial force is zero. To circumvent this problem and to avoid the use of different expressions for S_1 and S_2 for a different sign in axial forces, Lui and Chen [19] have proposed a set of expressions that use power-series expansions to approximate the stability functions. The power-series expressions have been shown to converge to a high degree of accuracy within the first ten terms of the series expansions. Alternatively, if the axial force in the member falls within the range $-2.0 \leq \rho \leq 2.0$, the following simplified expressions may be used to closely approximate the stability functions:

$$S_1 = 4 + \frac{2\pi^2\rho}{15} - \frac{(0.01\rho + 0.543)\rho^2}{4 + \rho} + \frac{(0.004\rho + 0.285)\rho^2}{8.183 + \rho} \quad (4)$$

$$S_2 = 2 - \frac{\pi^2\rho}{30} + \frac{(0.01\rho + 0.543)\rho^2}{4 + \rho} - \frac{(0.004\rho + 0.285)\rho^2}{8.183 + \rho} \quad (5)$$

Eqs. (4) and (5) are applicable for members in tension (positive P) and compression (negative P). For most practical applications, Eqs. (4) and (5) give an excellent agreement to the ‘exact’ expressions given by Eqs. (2) and (3). However, for ρ other than the range of $-2.0 \leq \rho \leq 2.0$, the conventional stability functions (Eqs. (2) and (3)) should be used. The stability function approach uses only one element per member and maintains accuracy in the element stiffness terms and in the recovery of element end forces for all ranges of axial loads.

2.4. Fixed end moments of a beam-column subjected to distributed lateral loads

The incremental fixed-end moments of a beam-column subjected to the axial force and linearly varying distributed lateral load shown in Fig. 1 may be written as

If $P < 0$ then,

$$\begin{aligned} \dot{M}_{FA} = & \frac{12\dot{w}_a(1 - \cos kL) + (kL)^2(\dot{w}_a + 2\dot{w}_b) - (kL)(9\dot{w}_a + 3\dot{w}_b)\sin kL}{12k^2(kL \cos(0.5kL) - 2 \sin(0.5kL))\sin(0.5kL)} \\ & + \frac{(kL)^2(2\dot{w}_a + \dot{w}_b)\cos kL}{12k^2(kL \cos(0.5kL) - 2 \sin(0.5kL))\sin(0.5kL)} \end{aligned} \quad (6a)$$

$$\begin{aligned} \dot{M}_{FB} = & \frac{12\dot{w}_b(\cos kL - 1) - (kL)^2(2\dot{w}_a + \dot{w}_b) + (kL)(3\dot{w}_a + 9\dot{w}_b)\sin kL}{12k^2(kL \cos(0.5kL) - 2 \sin(0.5kL))\sin(0.5kL)} \\ & - \frac{(kL)^2(\dot{w}_a + 2\dot{w}_b)\cos kL}{12k^2(kL \cos(0.5kL) - 2 \sin(0.5kL))\sin(0.5kL)} \end{aligned} \quad (6b)$$

If $P > 0$ then,

$$\dot{M}_{FA} = \frac{12\dot{w}_a(1 - \cosh kL) - (kL)^2(\dot{w}_a + 2\dot{w}_b) + (kL)(9\dot{w}_a + 3\dot{w}_b)\sinh kL}{12k^2(kL \cosh(0.5kL) - 2 \sinh(0.5kL))\sinh(0.5kL)} - \frac{(kL)^2(2\dot{w}_a + \dot{w}_b)\cosh kL}{12k^2(kL \cosh(0.5kL) - 2 \sinh(0.5kL))\sinh(0.5kL)} \tag{7a}$$

$$\dot{M}_{FB} = \frac{12\dot{w}_b(\cosh kL - 1) + (kL)^2(2\dot{w}_a + \dot{w}_b) - (kL)(3\dot{w}_a + 9\dot{w}_b)\sinh kL}{12k^2(kL \cosh(0.5kL) - 2 \sinh(0.5kL))\sinh(0.5kL)} + \frac{(kL)^2(\dot{w}_a + 2\dot{w}_b)\cosh kL}{12k^2(kL \cosh(0.5kL) - 2 \sinh(0.5kL))\sinh(0.5kL)} \tag{7b}$$

where $k = \sqrt{\frac{P}{EI}}$.

The numerical solutions obtained from Eqs. (6a), (6b), (7a) and (7b) are indeterminate when the axial force is zero. The following power series expansion are used:

$$\dot{M}_{FA} = -\frac{(3w_a + 2w_b)L^2}{60} + \frac{(19w_a + 16w_b)k^2L^4}{25,200} - \frac{(13w_a + 12w_b)k^4L^6}{756,000} \tag{8}$$

$$\dot{M}_{FB} = \frac{(2w_a + 3w_b)L^2}{60} - \frac{(16w_a + 19w_b)k^2L^4}{25,200} + \frac{(12w_a + 13w_b)k^4L^6}{756,000} \tag{9}$$

2.5. Space beam-column subjected to distributed lateral loads

The incremental force–displacement equation may be extended for a three-dimensional beam-column element as

$$\begin{pmatrix} \dot{P} \\ \dot{M}_{yA} \\ \dot{M}_{yB} \\ \dot{M}_{zA} \\ \dot{M}_{zB} \\ \dot{T} \end{pmatrix} = \begin{bmatrix} \frac{EA}{L} & 0 & 0 & 0 & 0 & 0 \\ 0 & S_1 \frac{EI_y}{L} & S_2 \frac{EI_y}{L} & 0 & 0 & 0 \\ 0 & S_2 \frac{EI_y}{L} & S_1 \frac{EI_y}{L} & 0 & 0 & 0 \\ 0 & 0 & 0 & S_3 \frac{EI_z}{L} & S_4 \frac{EI_z}{L} & 0 \\ 0 & 0 & 0 & S_4 \frac{EI_z}{L} & S_3 \frac{EI_z}{L} & 0 \\ 0 & 0 & 0 & 0 & 0 & \frac{GJ}{L} \end{bmatrix} \begin{pmatrix} \dot{\delta} \\ \dot{\theta}_{yA} \\ \dot{\theta}_{yB} \\ \dot{\theta}_{zA} \\ \dot{\theta}_{zB} \\ \dot{\phi} \end{pmatrix} + \begin{pmatrix} 0 \\ \dot{M}_{yFA} \\ \dot{M}_{yFB} \\ \dot{M}_{zFA} \\ \dot{M}_{zFB} \\ 0 \end{pmatrix} \tag{10}$$

where \dot{P} , \dot{M}_{yA} , \dot{M}_{yB} , \dot{M}_{zA} , \dot{M}_{zB} , and \dot{T} are incremental axial force, incremental end moments with respect to y and z axis and incremental torsion, respectively. $\dot{\delta}$, $\dot{\theta}_{yA}$, $\dot{\theta}_{yB}$, $\dot{\theta}_{zA}$, $\dot{\theta}_{zB}$, and $\dot{\phi}$ are the incremental axial displacement, the incremental joint rotations, and the incremental angle of twist. S_1 , S_2 , S_3 , and S_4 are the stability functions with respect to y and z axis, respectively.

2.6. CRC Tangent modulus model associated with residual stresses

The CRC tangent modulus concept is used to account for gradual yielding due to residual stresses along the length of axially loaded members between plastic hinges. The elastic modulus E (instead of moment of inertia I) is reduced to account for the reduction of the elastic portion of the cross-section since the reduction of the elastic modulus is easier to implement than a new moment of inertia for every different section. The rate of reduction in stiffness is different in the weak- and strong-directions, but this is not considered since the dramatic degradation of weak-axis stiffness is compensated for by the substantial weak-axis plastic strength [8]. This simplification makes the proposed method practical. From [18], the CRC E_t is written as

$$E_t = 1.0E \quad \text{for } P \leq 0.5P_y \tag{11a}$$

$$E_t = 4 \frac{P}{P_y} E \left(1 - \frac{P}{P_y} \right) \quad \text{for } P > 0.5P_y \tag{11b}$$

2.7. Parabolic function for gradual yielding due to flexure

The tangent modulus model is suitable for an element subjected to axial force, but not adequate for cases of both axial force and bending moment. A gradual stiffness degradation model for a plastic hinge is required to represent the partial plastification effects associated with bending. We shall introduce a softening plastic hinge model to represent the degradation from elastic to zero stiffness associated with development of a hinge. When softening plastic hinges are active at both ends of an element, the incremental force–displacement equation may be modified as

$$\begin{Bmatrix} \dot{P} \\ \dot{M}_{yA} \\ \dot{M}_{yB} \\ \dot{M}_{zA} \\ \dot{M}_{zB} \\ \dot{T} \end{Bmatrix} = \begin{bmatrix} \frac{E_t A}{L} & 0 & 0 & 0 & 0 & 0 \\ 0 & k_{iyy} & k_{ijy} & 0 & 0 & 0 \\ 0 & k_{ijy} & k_{jyy} & 0 & 0 & 0 \\ 0 & 0 & 0 & k_{iiz} & k_{ijz} & 0 \\ 0 & 0 & 0 & k_{ijz} & k_{jiz} & 0 \\ 0 & 0 & 0 & 0 & 0 & \frac{GJ}{L} \end{bmatrix} \begin{Bmatrix} \dot{\delta} \\ \dot{\theta}_{yA} \\ \dot{\theta}_{yB} \\ \dot{\theta}_{zA} \\ \dot{\theta}_{zB} \\ \dot{\phi} \end{Bmatrix} + \begin{Bmatrix} 0 \\ \dot{M}_{yFA} \\ \dot{M}_{yFB} \\ \dot{M}_{zFA} \\ \dot{M}_{zFB} \\ 0 \end{Bmatrix} \tag{12}$$

where

$$k_{iyy} = \eta_A \left(S_1 - \frac{S_2^2}{S_1} (1 - \eta_B) \right) \frac{E_t I_y}{L} \tag{13a}$$

$$k_{ijy} = \eta_A \eta_B S_2 \frac{E_t I_y}{L} \tag{13b}$$

$$k_{jyy} = \eta_B \left(S_1 - \frac{S_2^2}{S_1} (1 - \eta_A) \right) \frac{E_t I_y}{L} \quad (13c)$$

$$k_{iiz} = \eta_A \left(S_3 - \frac{S_4^2}{S_3} (1 - \eta_B) \right) \frac{E_t I_z}{L} \quad (13d)$$

$$k_{ijz} = \eta_A \eta_B S_4 \frac{E_t I_z}{L} \quad (13e)$$

$$k_{jjz} = \eta_B \left(S_3 - \frac{S_4^2}{S_3} (1 - \eta_A) \right) \frac{E_t I_z}{L} \quad (13f)$$

The terms η_A and η_B is a scalar parameter that allows for gradual inelastic stiffness reduction of the element associated with plastification at end A and B. This term is equal to 1.0 when the element is elastic, and zero when a plastic hinge is formed. The parameter η is assumed to vary according to the parabolic function:

$$\eta = 1.0 \quad \text{for } \alpha \leq 0.5 \quad (14a)$$

$$\eta = 4\alpha(1 - \alpha) \quad \text{for } \alpha > 0.5 \quad (14b)$$

where α is a force-state parameter that measures the magnitude of axial force and bending moment at the element end. The term α may be expressed by AISC-LRFD and Orbison, respectively:

2.7.1. AISC-LRFD

Based on AISC-LRFD bilinear interaction equation [20,21], the cross-section plastic strength of the beam-column member may be expressed

$$\alpha = \frac{P}{P_y} + \frac{8}{9} \frac{M_y}{M_{yp}} + \frac{8}{9} \frac{M_z}{M_{zp}} \quad \text{for } \frac{P}{P_y} \geq \frac{2}{9} \frac{M_y}{M_{yp}} + \frac{2}{9} \frac{M_z}{M_{zp}} \quad (15)$$

$$\alpha = \frac{P}{2P_y} + \frac{M_y}{M_{yp}} + \frac{M_z}{M_{zp}} \quad \text{for } \frac{P}{P_y} < \frac{2}{9} \frac{M_y}{M_{yp}} + \frac{2}{9} \frac{M_z}{M_{zp}} \quad (16)$$

2.7.2. Orbison

Orbison's full plastification surface [14] of cross-section is given by

$$\alpha = 1.15p^2 + m_z^2 + m_y^4 + 3.67p^2m_z^2 + 3.0p^6m_y^2 + 4.65m_z^4m_y^2 \quad (17)$$

Where $p = P/P_y$, $m_z = M_z/M_{pz}$ (strong-axis), $m_y = M_y/M_{py}$ (weak-axis).

Initial yielding is assumed to occur based on a yield surface that has the same shape as the full plastification surface and with the force-state parameter denoted as $\alpha_0 = 0.5$. If the forces change so the force point moves inside or along the initial yield surface, the element is assumed to remain fully elastic with no stiffness reduction. If the force point moves beyond the initial yield surface, the element stiffness is reduced to account for the effect of plastification at the element end.

2.8. Shear deformation

The stiffness coefficients should be modified to account for the effect of the additional flexural shear deformation in a beam-column element. The flexural flexibility matrix can be obtained by inverting the flexural stiffness matrix as

$$\begin{Bmatrix} \dot{\theta}_{MA} \\ \dot{\theta}_{MB} \end{Bmatrix} = \begin{bmatrix} \frac{k_{jj}}{k_{ii}k_{jj} - k_{ij}^2} & -\frac{k_{ij}}{k_{ii}k_{jj} - k_{ij}^2} \\ -\frac{k_{ij}}{k_{ii}k_{jj} - k_{ij}^2} & \frac{k_{ii}}{k_{ii}k_{jj} - k_{ij}^2} \end{bmatrix} \begin{Bmatrix} \dot{M}_A \\ \dot{M}_B \end{Bmatrix} \tag{18}$$

where k_{ii} , k_{ij} , and k_{jj} are the elements of stiffness matrix in a planar beam-column. $\dot{\theta}_{MA}$ and $\dot{\theta}_{MB}$ are the incremental slope of the neutral axis due to bending moment. The flexibility matrix corresponding to flexural shear deformation may be written as

$$\begin{Bmatrix} \dot{\theta}_{SA} \\ \dot{\theta}_{SB} \end{Bmatrix} = \begin{bmatrix} \frac{1}{GA_s} & \frac{1}{GA_s} \\ \frac{1}{GA_s} & \frac{1}{GA_s} \end{bmatrix} \begin{Bmatrix} \dot{M}_A \\ \dot{M}_B \end{Bmatrix} \tag{19}$$

where GA_s and L are shear rigidity and length of the beam-column, respectively. Incremental rotation at the A and B is obtained by combining Eqs. (18) and (19) as

$$\begin{Bmatrix} \dot{\theta}_A \\ \dot{\theta}_B \end{Bmatrix} = \begin{Bmatrix} \dot{\theta}_{MA} \\ \dot{\theta}_{MB} \end{Bmatrix} + \begin{Bmatrix} \dot{\theta}_{SA} \\ \dot{\theta}_{SB} \end{Bmatrix} \tag{20}$$

The incremental force–displacement relationship including flexural shear deformation is obtained by inverting the flexibility matrix as

$$\begin{Bmatrix} \dot{M}_A \\ \dot{M}_B \end{Bmatrix} = \begin{bmatrix} \frac{k_{ii}k_{jj} - k_{ij}^2 + k_{ii}A_sGL}{k_{ii} + k_{jj} + 2k_{ij} + A_sGL} & \frac{-k_{ii}k_{jj} + k_{ij}^2 + k_{ij}A_sGL}{k_{ii} + k_{jj} + 2k_{ij} + A_sGL} \\ \frac{-k_{ii}k_{jj} + k_{ij}^2 + k_{ij}A_sGL}{k_{ii} + k_{jj} + 2k_{ij} + A_sGL} & \frac{k_{ii}k_{jj} - k_{ij}^2 + k_{jj}A_sGL}{k_{ii} + k_{jj} + 2k_{ij} + A_sGL} \end{bmatrix} \begin{Bmatrix} \dot{\theta}_A \\ \dot{\theta}_B \end{Bmatrix} \tag{21}$$

The incremental force–displacement equation may be expanded for the three-dimensional beam-column element as

$$\begin{Bmatrix} \dot{P} \\ \dot{M}_{yA} \\ \dot{M}_{yB} \\ \dot{M}_{zA} \\ \dot{M}_{zB} \\ \dot{T} \end{Bmatrix} = \begin{bmatrix} \frac{EA}{L} & 0 & 0 & 0 & 0 & 0 \\ 0 & C_{iiv} & C_{ijv} & 0 & 0 & 0 \\ 0 & C_{ijv} & C_{jyv} & 0 & 0 & 0 \\ 0 & 0 & 0 & C_{iiz} & C_{ijz} & 0 \\ 0 & 0 & 0 & C_{ijz} & C_{jiz} & 0 \\ 0 & 0 & 0 & 0 & 0 & \frac{GJ}{L} \end{bmatrix} \begin{Bmatrix} \dot{\delta} \\ \dot{\theta}_{yA} \\ \dot{\theta}_{yB} \\ \dot{\theta}_{zA} \\ \dot{\theta}_{zB} \\ \dot{\phi} \end{Bmatrix} + \begin{Bmatrix} 0 \\ \dot{M}_{yFA} \\ \dot{M}_{yFB} \\ \dot{M}_{zFA} \\ \dot{M}_{zFB} \\ 0 \end{Bmatrix} \tag{22}$$

in which

$$C_{iyy} = \frac{k_{iyy}k_{jyy} - k_{ijy}^2 + k_{iyy}A_{sz}GL}{k_{iyy} + k_{jyy} + 2k_{ijy} + A_{sz}GL} \quad (23a)$$

$$C_{ijy} = \frac{-k_{iyy}k_{jyy} + k_{ijy}^2 + k_{ijy}A_{sz}GL}{k_{iyy} + k_{jyy} + 2k_{ijy} + A_{sz}GL} \quad (23b)$$

$$C_{jyy} = \frac{k_{iyy}k_{jyy} - k_{ijy}^2 + k_{jyy}A_{sz}GL}{k_{iyy} + k_{jyy} + 2k_{ijy} + A_{sz}GL} \quad (23c)$$

$$C_{iiz} = \frac{k_{iiz}k_{jiz} - k_{ijz}^2 + k_{iiz}A_{sy}GL}{k_{iiz} + k_{jiz} + 2k_{ijz} + A_{sy}GL} \quad (23d)$$

$$C_{ijz} = \frac{-k_{iiz}k_{jiz} + k_{ijz}^2 + k_{ijz}A_{sy}GL}{k_{iiz} + k_{jiz} + 2k_{ijz} + A_{sy}GL} \quad (23e)$$

$$C_{jiz} = \frac{k_{iiz}k_{jiz} - k_{ijz}^2 + k_{jiz}A_{sy}GL}{k_{iiz} + k_{jiz} + 2k_{ijz} + A_{sy}GL} \quad (23f)$$

where A_{sy} and A_{sz} are the effective shear flexure shear areas with respect to y and z axes, respectively.

The incremental force–displacement relationship from Eq. (22) may be symbolically written as

$$\{\dot{f}_e\} = [K_e]\{\dot{d}_e\} \quad (24)$$

in which $\{\dot{f}_e\}$ and $\{\dot{d}_e\}$ are the incremental end force and incremental displacement, and $[K_e]$ is the tangent stiffness matrix.

2.9. Element stiffness matrix accounting for $P-\Delta$ effect

The incremental end forces and end displacements used in Eq. (22) are shown in Fig. 2(a). The sign convention for the positive directions of element end forces and end displacements of a beam-column element is shown in Fig. 2(b). By comparing the two figures, we can express the equilibrium and kinematic relationships in symbolic form as

$$\{\dot{f}_n\} = [T]_{6 \times 12}^T \{\dot{f}_e\} \quad (25)$$

$$\{\dot{d}_e\} = [T]_{6 \times 12} \{\dot{d}_L\} \quad (26)$$

$\{\dot{f}_n\}$ and $\{\dot{d}_L\}$ are the incremental end force and displacement vectors of a beam-column element expressed as

$$\{\dot{f}_n\}^T = \{r_{n1} \ r_{n2} \ r_{n3} \ r_{n4} \ r_{n5} \ r_{n6} \ r_{n7} \ r_{n8} \ r_{n9} \ r_{n10} \ r_{n11} \ r_{n12}\} \quad (27a)$$

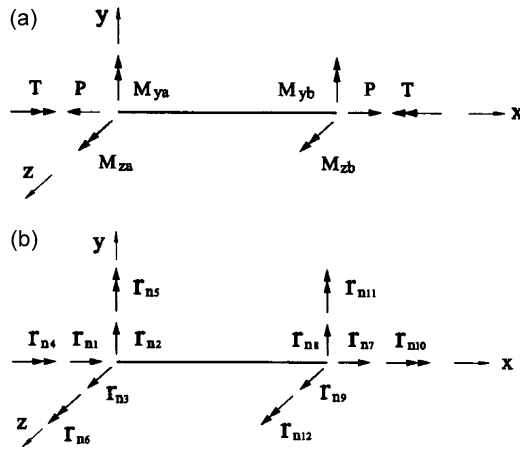


Fig. 2. Notation of element end forces and displacements.

$$\{\dot{d}_L\}^T = \{d_1 \quad d_2 \quad d_3 \quad d_4 \quad d_5 \quad d_6 \quad d_7 \quad d_8 \quad d_9 \quad d_{10} \quad d_{11} \quad d_{12}\} \quad (27b)$$

$\{\dot{f}_e\}$ and $\{\dot{d}_e\}$ are the incremental end force and displacement vectors in Eq. (22). $[T]_{6 \times 12}$ is a transformation matrix written as

$$[T]_{6 \times 12} = \begin{bmatrix} -1 & 0 & 0 & 0 & 0 & 0 & 1 & 0 & 0 & 0 & 0 & 0 \\ 0 & 0 & -\frac{1}{L} & 0 & 1 & 0 & 0 & 0 & \frac{1}{L} & 0 & 0 & 0 \\ 0 & 0 & -\frac{1}{L} & 0 & 0 & 0 & 0 & 0 & \frac{1}{L} & 0 & 1 & 0 \\ 0 & \frac{1}{L} & 0 & 0 & 0 & 1 & 0 & -\frac{1}{L} & 0 & 0 & 0 & 0 \\ 0 & \frac{1}{L} & 0 & 0 & 0 & 0 & 0 & -\frac{1}{L} & 0 & 0 & 0 & 1 \\ 0 & 0 & 0 & 1 & 0 & 0 & 0 & 0 & 0 & -1 & 0 & 0 \end{bmatrix}. \quad (28)$$

Using the transformation matrix by equilibrium and kinematic relations, the incremental force–displacement relationship of a beam-column element may be written as

$$\{\dot{f}_n\} = [K_n]\{\dot{d}_L\}. \quad (29)$$

$[K_n]$ is the element stiffness matrix expressed as

$$[K_n]_{12 \times 12} = [T]_{6 \times 12}^T [K_e]_{6 \times 6} [T]_{6 \times 12}. \quad (30)$$

Eq. (30) can be subgrouped as

$$[K_n]_{12 \times 12} = \begin{bmatrix} [K_n]_1 & [K_n]_2 \\ [K_n]_2^T & [K_n]_3 \end{bmatrix} \quad (31)$$

where

$$[K_n]_1 = \begin{bmatrix} a & 0 & 0 & 0 & 0 & 0 \\ 0 & b & 0 & 0 & 0 & c \\ 0 & 0 & d & 0 & -e & 0 \\ 0 & 0 & 0 & f & 0 & 0 \\ 0 & 0 & -e & 0 & g & 0 \\ 0 & c & 0 & 0 & 0 & h \end{bmatrix} \quad (32a)$$

$$[K_n]_2 = \begin{bmatrix} -a & 0 & 0 & 0 & 0 & 0 \\ 0 & -b & 0 & 0 & 0 & c \\ 0 & 0 & -d & 0 & -e & 0 \\ 0 & 0 & 0 & -f & 0 & 0 \\ 0 & 0 & e & 0 & i & 0 \\ 0 & -c & 0 & 0 & 0 & j \end{bmatrix} \quad (32b)$$

$$[K_n]_3 = \begin{bmatrix} a & 0 & 0 & 0 & 0 & 0 \\ 0 & b & 0 & 0 & 0 & -c \\ 0 & 0 & d & 0 & e & 0 \\ 0 & 0 & 0 & f & 0 & 0 \\ 0 & 0 & e & 0 & m & 0 \\ 0 & c & 0 & 0 & 0 & n \end{bmatrix} \quad (32c)$$

where

$$\begin{aligned} a &= \frac{E_t A}{L}, & b &= \frac{C_{iiz} + 2C_{ijz} + C_{jzj}}{L^2}, & c &= \frac{C_{iiz} + C_{ijz}}{L}, \\ \sqrt{d} &= \frac{C_{iyy} + 2C_{ijy} + C_{jyy}}{L^2}, & e &= \frac{C_{iyy} + C_{ijy}}{L}, & f &= \frac{GJ}{L}, & g &= C_{iyy}, \\ h &= C_{iiz}, & \sqrt{i} &= C_{ijy}, & j &= C_{ijz}, & m &= C_{jyy}, & n &= C_{jzj} \end{aligned} \quad (33)$$

Eq. (31) is used to enforce no sideways in the element. If the element is permitted to sway, an additional axial and shear forces will be induced in the element. We can relate this additional axial and shear forces due to an element sway to the element end

displacements as

$$\{\dot{f}_s\} = [K_s]\{\dot{d}_L\}. \tag{34}$$

where $\{\dot{f}_s\}$, $\{\dot{d}_L\}$, and $[K_s]$ are incremental end force vector, incremental end displacement vector, and the element stiffness matrix. They may be written as

$$\{\dot{f}_s\}^T = \{r_{s1} \ r_{s2} \ r_{s3} \ r_{s4} \ r_{s5} \ r_{s6} \ r_{s7} \ r_{s8} \ r_{s9} \ r_{s10} \ r_{s11} \ r_{s12}\} \tag{35a}$$

$$\{\dot{d}_L\}^T = \{d_1 \ d_2 \ d_3 \ d_4 \ d_5 \ d_6 \ d_7 \ d_8 \ d_9 \ d_{10} \ d_{11} \ d_{12}\} \tag{35b}$$

$$[K_s]_{12 \times 12} = \begin{bmatrix} [K_s]_s & -[K_s]_s \\ -[K_s]_s^T & [K_s]_s \end{bmatrix} \tag{35c}$$

where

$$[K_s]_s = \begin{bmatrix} 0 & a & -b & 0 & 0 & 0 \\ a & c & 0 & 0 & 0 & 0 \\ -b & 0 & c & 0 & 0 & 0 \\ 0 & 0 & 0 & 0 & 0 & 0 \\ 0 & 0 & 0 & 0 & 0 & 0 \\ 0 & 0 & 0 & 0 & 0 & 0 \end{bmatrix} \tag{36}$$

and

$$a = \frac{M_{zA} + M_{zB}}{L^2} \quad b = \frac{M_{yA} + M_{yB}}{L^2} \quad c = \frac{P}{L}. \tag{37}$$

By combining Eqs. (29) and (34), we obtain the incremental force–displacement relationship as

$$\{\dot{f}_L\} = [K]_{local}\{\dot{d}_L\} \tag{38}$$

where

$$\{\dot{f}_L\} = \{\dot{f}_n\} + \{\dot{f}_s\} \tag{39}$$

$$[K]_{local} = [K_n] + [K_s]. \tag{40}$$

2.10. Moving node strategy

When a member is subjected to distributed lateral loads, a plastic hinge may occur at the member ends or within the member. The plastic hinge occurred within the member is called an internal plastic hinge. The exact location of the internal plastic hinge varies depending on the member end forces and distributed lateral loads. In this study, a member has two elements and three nodal points shown in Fig. 3. This internal nodal point, that is moving node, traces the location of maximum moment within a member where might be

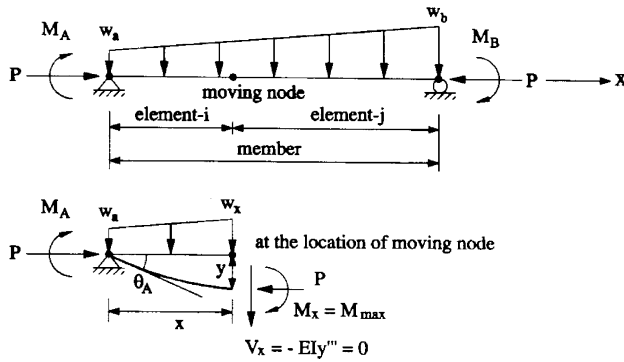


Fig. 3. Beam-column member with moving node.

the location of the plastic hinge when the member forces get to the yield surface. The location of the moving node is calculated considering both 1st-order moment (primary bending moment) and 2nd-order moment ($P - \delta$ moment). The nonlinear displacement of the member may be written as

If $P < 0$ then,

$$\begin{aligned}
 y = & \left(-\frac{M_B + M_A \cos kL}{EI k^2 \sin kL} + \frac{w_b - w_a \cos kL}{EI k^4 \sin kL} \right) \sin kx \\
 & + \left(\frac{w_a}{EI k^4} + \frac{M_A}{EI k^2} \right) \cos kx + \frac{w_b - w_a}{6LEI k^2} x^3 + \frac{w_a}{2EI k^2} x^2 - \frac{L(2w_a + w_b)}{6EI k^2} x \\
 & + \frac{M_A + M_B}{LEI k^2} x - \frac{w_b - w_a}{LEI k^4} x - \frac{w_a}{EI k^4} - \frac{M_A}{EI k^2}
 \end{aligned} \tag{41a}$$

If $P > 0$ then,

$$\begin{aligned}
 y = & \left(\frac{M_B + M_A \cosh kL}{EI k^2 \sinh kL} + \frac{w_b - w_a \cosh kL}{EI k^4 \sinh kL} \right) \sinh kx \\
 & + \left(\frac{w_a}{EI k^4} - \frac{M_A}{EI k^2} \right) \cosh kx - \frac{w_b - w_a}{6LEI k^2} x^3 - \frac{w_a}{2EI k^2} x^2 + \frac{L(2w_a + w_b)}{6EI k^2} x \\
 & - \frac{M_A + M_B}{LEI k^2} x - \frac{w_b - w_a}{LEI k^4} x - \frac{w_a}{EI k^4} + \frac{M_A}{EI k^2}
 \end{aligned} \tag{41b}$$

And the shear force may be written as

$$V_x = -EI y''' \tag{42}$$

where

for $P < 0$

$$y''' = \left(\frac{k(M_B + M_A \cos kL)}{EI \sin kL} - \frac{w_b - w_a^a \cos kL}{EI k \sin kL} \right) \cos kx + \frac{w_a + kM_A}{EI} \sin kx + \frac{w_b - w_a}{LEIk^2} \tag{43a}$$

for $P > 0$

$$y''' = \left(\frac{k(M_B + M_A \cosh kL)}{EI \sinh kL} + \frac{w_b - w_a^a \cosh kL}{EI k \sinh kL} \right) \cosh kx + \frac{w_a - kM_A}{EI} \sinh kx - \frac{w_b - w_a}{LEIk^2} \tag{43b}$$

The location of moving node may be obtained by setting the shear force equal to zero. The numerical technique of the bi-section method is used to calculate the location of x . Fig. 4 shows the flowchart of the proposed method.

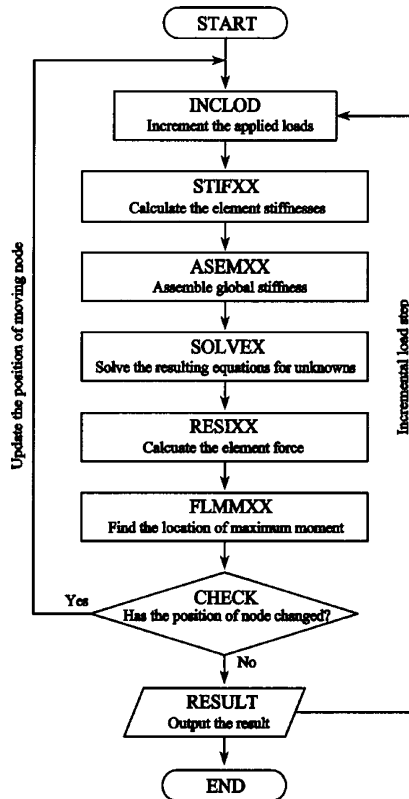


Fig. 4. Flowchart of the proposed method.

2.11. Numerical implementation

The simple incremental method, as a direct nonlinear solution technique, is used in the analysis. Its numerical procedure is straightforward in concept and implementation. The advantage of this method is its computational efficiency. This is especially true when the structure is loaded into the inelastic region since tracing the hinge-by-hinge formation is required in the element stiffness formulation. For a finite increment size, this approach only approximates the nonlinear structural response, and equilibrium between the external applied loads and the internal element forces is not satisfied. To avoid this, an improved incremental method is used in this program. The applied load increment is automatically reduced to minimize the error when the change in the element stiffness parameter ($\Delta\eta$) exceeds a defined tolerance.

3. Verifications

In the open literature, no available benchmark problems of space frames subjected to distributed loads with moving node are available for verification study. One way to verify the proposed analysis is to make separate verifications for the nonlinear behavior of the space frame and for the effect of moving node.

3.1. Nonlinear behavior of space rigid frame

This verification study is performed to compare the load–displacement of the proposed analysis method with that obtained by [14,16]. Fig. 5 shows a six-story space frame. The yield strength of all members is 250 MPa (36 ksi) and Young’s modulus is 206,850 MPa

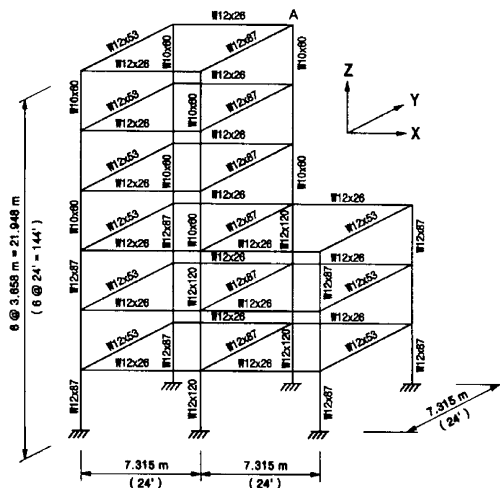


Fig. 5. Six-story space frame.

Table 1
Analysis result considering shear deformation

	Method		
	Proposed		Liew's
Plastic strength surface	LRFD	Orbison	Orbison
Ultimate load factor	1.990	2.057	2.062
Displacement at A in y-direction	208 mm	219 mm	250 mm

Table 2
Analysis result ignoring shear deformation

	Method		
	Proposed		Orbison's
Plastic strength surface	LRFD	Orbison	Orbison
Ultimate load factor	1.997	2.066	2.059
Displacement at A in y-direction	199 mm	208 mm	247 mm

(30,000 ksi). Uniform floor pressure of 4.8 kN/m^2 (100 psf) is converted into equivalent concentrated loads applied on the top of the columns. Wind loads are simulated by point loads of 26.7 kN (6 kips) in the Y-direction at every beam-column joints.

The load–displacements calculated by the proposed analysis compare well with those of Liew and Tang (considering shear deformations) and Orbison (ignoring shear deformations) (Tables 1 and 2, and Fig. 6). The ultimate load factors calculated from the proposed analysis are 2.057 and 2.066. These values are very close to 2.062 and 2.059 calculated by Liew and Tang and Orbison, respectively.

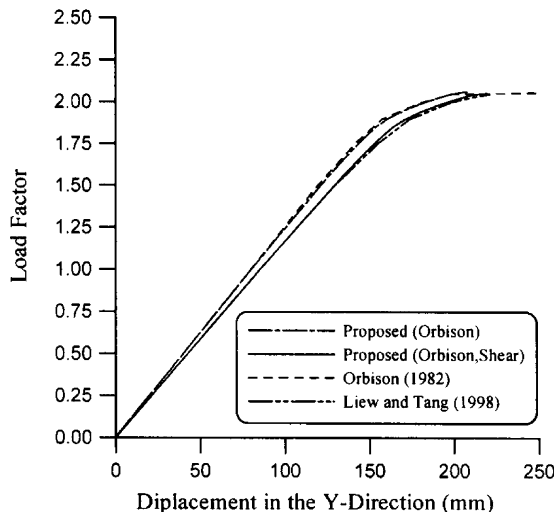


Fig. 6. Comparison of load–displacement of six-story space frame.

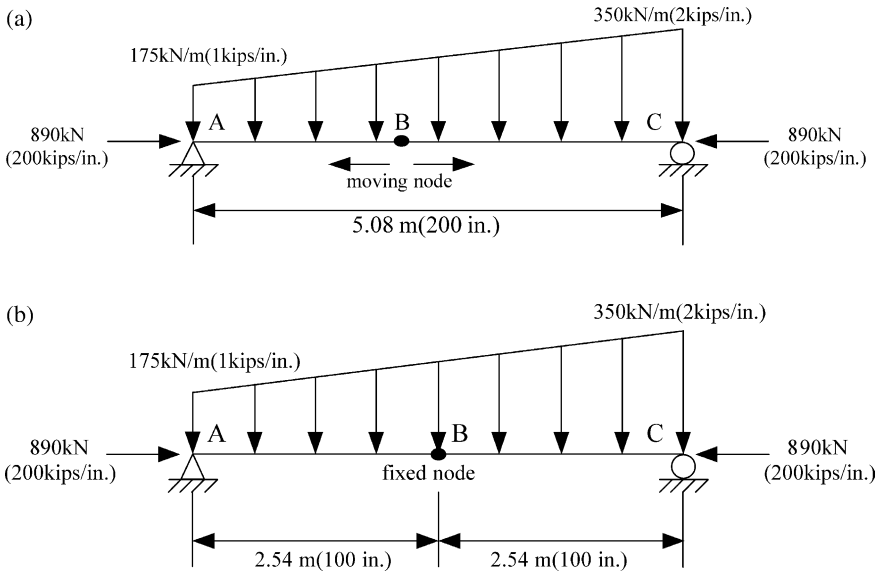


Fig. 7. Simply supported beam-column. (a) Moving node. (b) Fixed node.

3.2. Effects of moving node

3.2.1. Simply supported beam-column

Fig. 7 shows a simply supported beam-column subjected to linearly varying distributed lateral loads. W16×77 of A36 steel is used for the analysis. Three analyses are carried out: (1) second-order inelastic analysis with moving node (proposed); (2) second-order inelastic analysis with fixed node in mid-span; (3) plastic zone analysis [22]. While the analyses (1) and (3) use the moving node strategy tracing the maximum moment location, the analysis (2) uses the fixed node not moving from the center of a member. The ultimate load factors and the moving node locations are compared in Table 3. The ultimate load factors obtained from the analyses (1), (2), and (3) are 0.642, 0.644, and 0.666, respectively. The proposed analysis predicts precisely the ultimate load factor compared with ABAQUS (error is 3.7%). While the maximum moment locations obtained from the proposed analysis and ABAQUS are 2.68 and 2.67 m from point A with difference 0.4%, the analysis (2) show 4.8% difference in the location compared to the ABAQUS result.

Table 3
Analysis result of simply supported beam-column

	Method		
	Moving node method	Fixed node method	ABAQUS
Ultimate load factor	0.642	0.644	0.666
Location of moving node from A	2.68 m	2.54 m	2.67 m

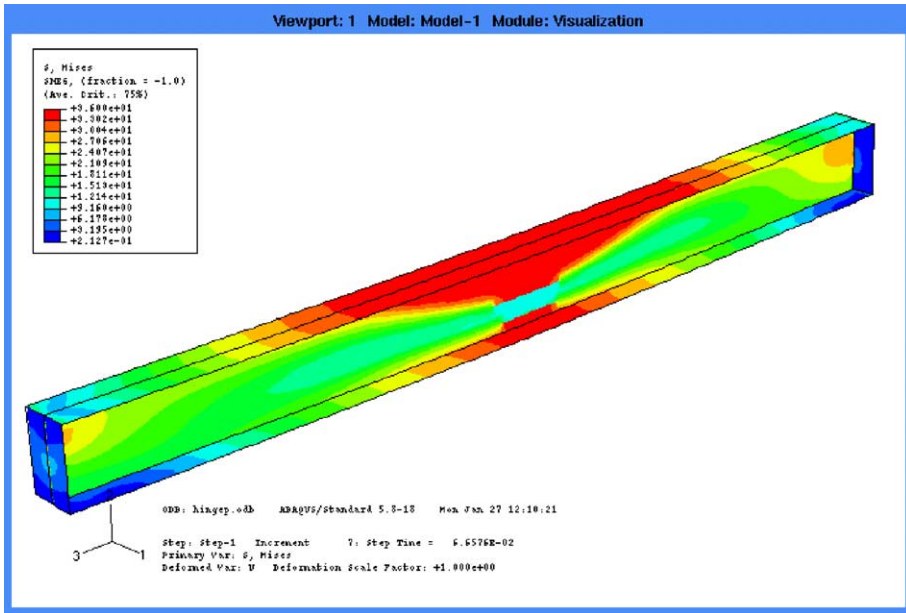


Fig. 8. Stress contour of simply supported beam-column.

Stress contour obtained by ABAQUS is shown in Fig. 8. The load–displacements obtained by three analyses are shown in Fig. 9.

3.2.2. Fixed-hinged beam-column

Fig. 10 shows a fixed-hinged beam-column subjected to linearly varying distributed lateral load. $W16 \times 77$ of A36 steel is used for the analysis. Three analyses are carried out: (1) second-order inelastic analysis with moving node (proposed); (2) second-order

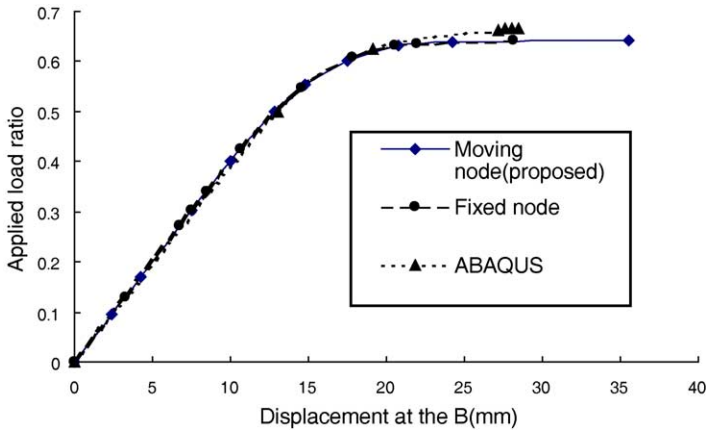


Fig. 9. Load–displacement of simply supported beam-column.

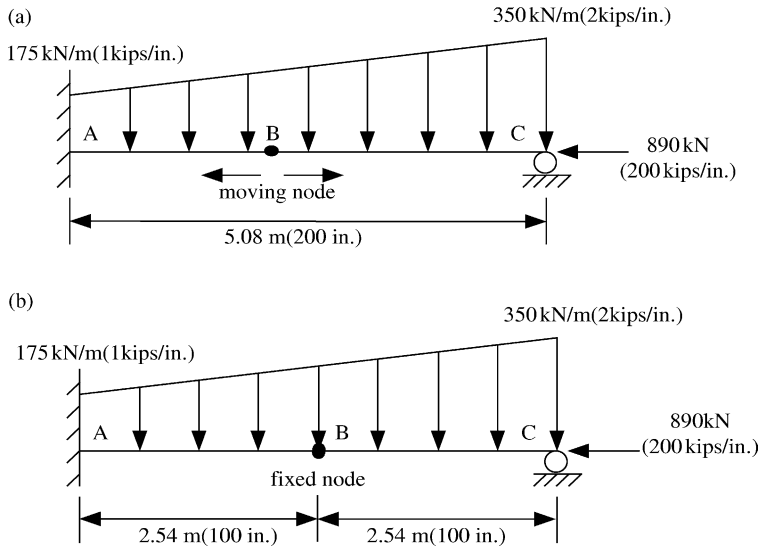


Fig. 10. Fixed-hinged beam-column (a) Moving node, (b) Fixed node.

inelastic analysis with fixed node in mid-span; (3) plastic zone analysis [22]. While the analyses (1) and (3) use the moving node strategy tracing the maximum moment location, the analysis (2) uses the fixed node not moving from the center of a member. The ultimate load factors and the moving node locations are compared in Table 4. The ultimate load factors obtained from the analyses (1), (2), and (3) are 0.905, 0.933, and 0.867, respectively. The proposed analysis predicts precisely the ultimate load factor with the error of 4.4% better than analysis (2) with the error 7.6%, compared with ABAQUS. While the maximum moment locations obtained from the proposed analysis and ABAQUS 3.37 and 3.17 m from point A with difference 6.3%, the analysis (2) show 19.8% difference in the location compared to the ABAQUS result. Stress contour obtained by ABAQUS is shown in Fig. 11. The load–displacements obtained by three analyses are shown in Fig. 12.

3.2.3. Vogel's six-story frame

Fig. 13 shows a Vogel's six-story frame. The yield strength of all members is 235 N/mm² and Young's modulus is 205 kN/mm². Three analyses are carried out: (1)

Table 4
Analysis result of fixed-hinged beam-column

	Method		
	Moving node method	Fixed node method	ABAQUS
Ultimate load factor	0.905	0.933	0.867
Location of moving node from A	3.37 m	2.54 m	3.17 m

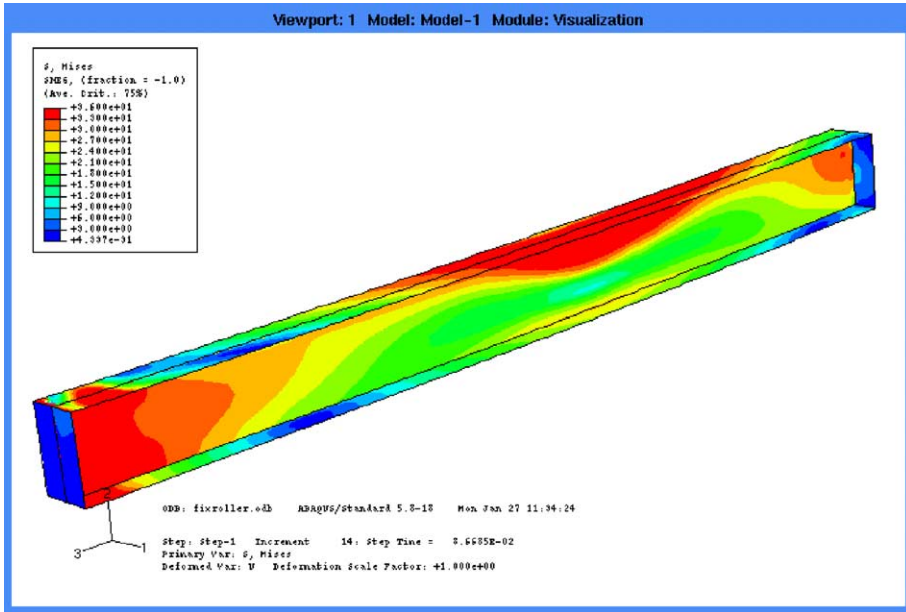


Fig. 11. Stress contour of fixed-hinged beam-column.

second-order inelastic analysis considering distributed lateral load with moving node (proposed); (2) second-order inelastic analysis using equivalent concentrated load with 4 elements per member; (3) second-order inelastic analysis using equivalent concentrated load with 2 elements per member. The load–displacements calculated by three analyses and Vogel’s plastic zone analysis are compared in Fig. 14. The ultimate load factors calculated by four analyses are 1.131, 1.090, 1.088, and 1.111, respectively. The proposed

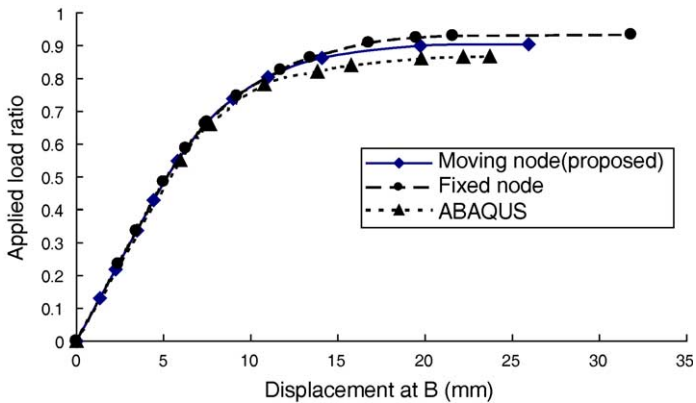


Fig. 12. Load–displacement of fixed-hinged beam-column.

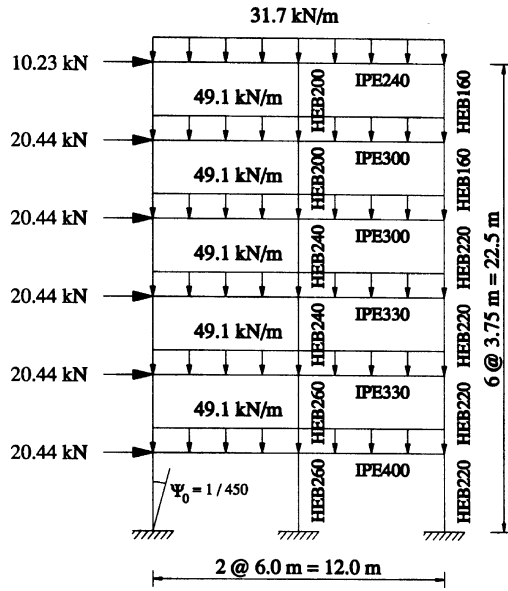


Fig. 13. Vogel's frame.

analysis predicts a very close ultimate load factor compared with Vogel's. While the ultimate load factors calculated by analysis (2) and (3) are very close to that of proposed analysis, the displacements of analysis (2) and (3) are considerably different from that of proposed analysis. The locations of moving node calculated by proposed analysis are shown in Fig. 15.

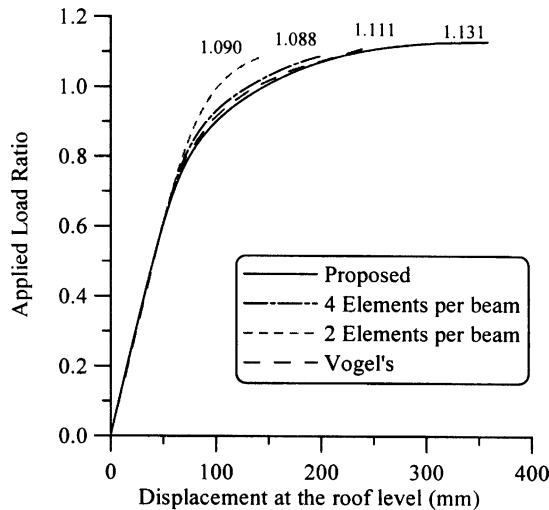


Fig. 14. Load–displacement of Vogel's frame.

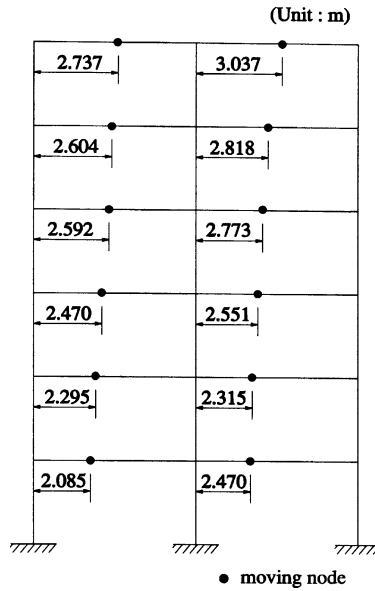


Fig. 15. Location of moving node.

4. Case study

Fig. 16 shows a two-story frame subjected to the distributed gravity load and the concentrated wind load. Each story is 4.572 m (180 in.) high, 6.096 m (240 in.) wide in the x-direction, and 4.573 m (180 in.) wide in the y-direction. The member sizes of beams and columns are W27×94 and W14×43, respectively. The yield stress used is 250 MPa (36 ksi) and Young’s modulus is 200,000 MPa (29,000 ksi). Two analyses are carried out:

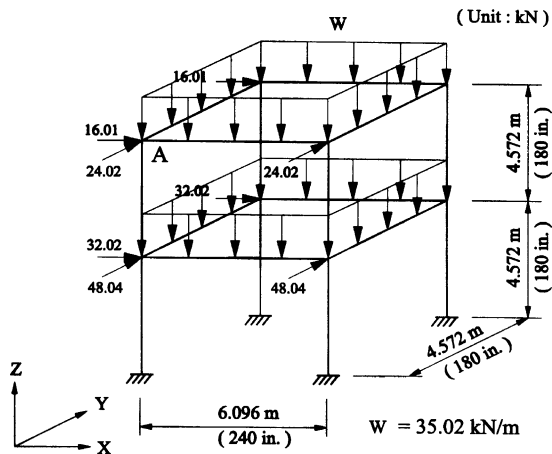


Fig. 16. Two-story frame.

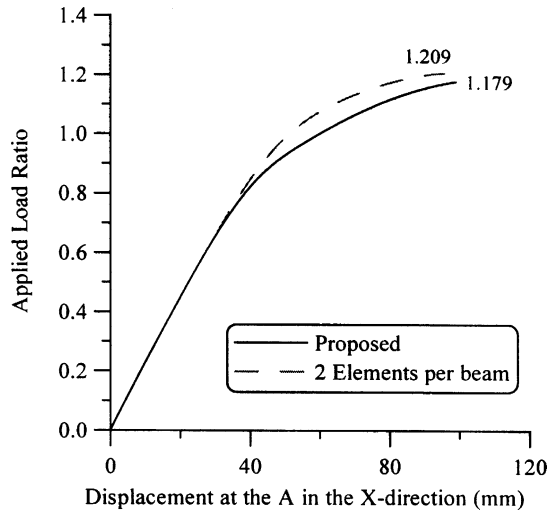


Fig. 17. Load–displacement of two-story frame in the *x*-direction.

(1) second-order inelastic analysis considering distributed lateral load with moving node (proposed); (2) second-order inelastic analysis using converted concentrated load with 2 elements per beam. The load–displacements in *x* and *y* direction calculated by two analyses are compared in Figs. 17 and 18. The ultimate load factors calculated by two analyses are very close as 1.179 and 1.209, respectively. However, the displacements between two analyses are considerably different up to about 20%.

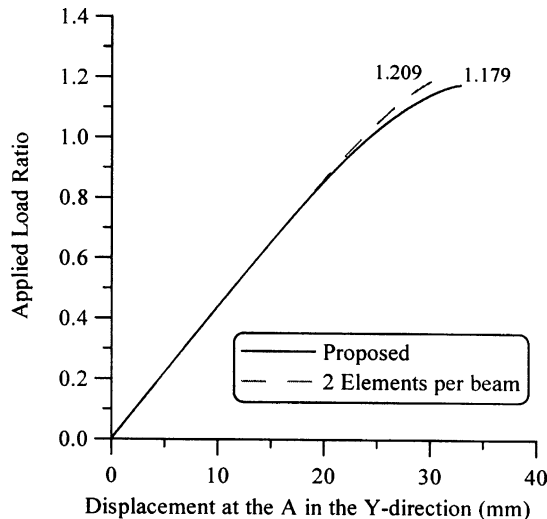


Fig. 18. Load–displacement of two-story frame in the *y*-direction.

5. Conclusions

In this paper, a practical second-order inelastic analysis of three-dimensional steel frames subjected to linearly varying distributed lateral loads has been developed. The conclusions of this study are as follows.

- (1) The proposed analysis can practically account for all key factors influencing steel frame behavior: gradual yielding associated with flexure and residual stresses and second-order effect.
- (2) Stability functions enable only one or two elements per member to capture second-order effects which make the proposed analysis practical.
- (3) The CRC tangent modulus and softening plastic hinge model consisting of member forces predict inelastic behavior reasonably well.
- (4) For Orbison's six-story space frame, the load–displacement from the proposed analysis compares well with Orbison's ignoring shear deformations and Liew's considering shear deformations.
- (5) When compared to plastic zone analysis, the location of the internal plastic hinge and the ultimate load factor are accurately captured using moving node strategy.
- (6) While the second-order inelastic analyses with the moving node and fixed node show small difference of 3% in the ultimate load factors in case of the fixed-hinged beam-column, they show big difference of up to 20% in the displacement for the case study.
- (7) The proposed analysis can be used in lieu of the costly plastic zone analysis.

Acknowledgements

The work presented in this paper was supported by the National Research Laboratory Program of the Ministry of Science and Technology in Korea. The authors appreciate the financial support.

References

- [1] Clarke MJ, Bridge RQ, Hancock GJ, Trahair NS. Benchmarking and verification of second-order elastic and inelastic frame analysis programs. In: White DW, Chen WF, editors. SSRC TG 29 workshop and nomograph on plastic hinge based methods for advanced analysis and design of steel frames. SSRC TG 29 workshop and nomograph on plastic hinge based methods for advanced analysis and design of steel frames. Bethlehem, PA: SSRC, Lehigh University; 1992.
- [2] El-Zanaty M, Murray D, Bjorhovde R. Inelastic behavior of multistory steel frames. Structural Engineering Report No. 83. Alberta, Canada: University of Alberta; 1980.
- [3] Vogel U. Calibrating frames. *Stahlbau* 1985;10:1–7.
- [4] White, DW. Material and geometric nonlinear analysis of local planar behavior in steel frames using iterative computer graphics, MS Thesis, Cornell University, Ithaca, NY; 1985: 281 p.
- [5] Liew JYR, White DW, Chen WF. Second-order refined plastic hinge analysis of frame design: part 1. *J Struct Eng, ASCE* 1993;119(11):3196–216.
- [6] Kim SE, Chen WF. Practical advanced analysis for braced steel frame design. *J Struct Eng, ASCE* 1996; 122(11):1266–74.

- [7] Kim SE, Chen WF. Practical advanced analysis for unbraced steel frame design. *J Struct Eng, ASCE* 1996; 122(11):1259–65.
- [8] Chen WF, Kim SE. LRFD steel design using advanced analysis. Boca Raton, FL: CRC Press; 1997.
- [9] Kim SE, Lee DH. Second-order distributed plasticity analysis of space steel frames. *Eng Struct* 2002;24: 735–44.
- [10] Kim SE, Lee JH, Park JS. 3-D second-order plastic-hinge analysis accounting for lateral torsional buckling. *Solids Struct* 2002;39:2109–28.
- [11] Kim SE, Choi SH, Ma SS. Performance based design of steel arch bridges using practical inelastic nonlinear analysis. *J Construct Steel Res* 2003;59:91–108.
- [12] Kim SE, Lee JH, Park JS. 3-D second-order plastic-hinge analysis accounting for local buckling. *Eng Struct* 2003;25(1):81–90.
- [13] Kim SE, Lee JS, Choi SH, Kim CS. Practical second-order inelastic analysis for steel frames subjected to distributed load. *Eng. Struct* 2004;26:51–61.
- [14] Orbison JG. Nonlinear static analysis of three-dimensional steel frames, Report No. 82-6. Ithaca, New York: Department of Structural Engineering, Cornell University; 1982.
- [15] Prakash V, Powell GH. DRAIN-3DX: Base program user guide, version 1.10, a Computer Program distributed by NISEE/Computer Applications, Department of Civil Engineering, University of California, Berkeley; 1993.
- [16] Liew JY, Tang LK. Nonlinear refined plastic hinge analysis of space frame structures. Research Report No. CE027/98. Singapore: Department of Civil Engineering, National University of Singapore; 1998.
- [17] Wong MB. Effects of linearly varying distributed load on the collapse behavior of frames. *Comput Struct* 1996;61(5):909–14.
- [18] Chen WF, Lui EM. Stability design of steel frames. Boca Raton, FL: CRC Press; 1992. 380 p..
- [19] Lui EM, Chen WF. Analysis and behavior of flexibly jointed frames. *Eng Struct* 1986;8:107–18.
- [20] AISC. Load and resistance factor design specification, 2nd ed. Chicago, IL: AISC; 1993.
- [21] Kanchanalai T. The design and behavior of beam-columns in unbraced steel frames. AISI Project No. 189, Report No. 2. Austin, TX: Civil Engineering/structures Research Lab., University of Texas; 1977: 300p.
- [22] ABAQUS. ABAQUS standard user's manual version 5.8, vol. I. Pawtucket, RI: Hibbit, Karlsson and Sorensen; 1998.